Mesospheric temperature inversions observed from long-term lidar measurements at mid- and low-latitudes.

Thierry Leblanc [a], I. Stuart McDermid [a], Philippe Keckhut [b], Alain Hauchecorne [b]

[a] JPL, California Institute of Technology, Table Mountain Facility, Wrightwood, CA 92397

[b] Service d'Aéronomie du CNRS, 91371 Verrières-le-Buisson, France

ABSTRACT

Results from new observations of mesospheric temperature inversion layers using long-term lidar measurements at mid- and low-latitudes are presented. Observations of inversions above Table Mountain, California, (34.4°N) and Mauna Loa, Hawaii, (19.5°N) are in very good agreement with previous lidar and satellite observations. At least two distinct types of events have been observed. The winter inversions occur near 70 km altitude at midlatitudes in December-January and about 1-2 months later at subtropical latitudes. The tidal signature in the middle atmospheric thermal structure has been investigated using more than 140 hours of nighttime lidar measurements at TMF during January 1997 and February 1998. The temperature profiles (30-85 km) revealed the presence of persistent mesospheric inversions around 65-70 km altitude with a clear Local-Solar-Time (LST) dependence. Also, some higher altitude inversions (80-85 km) have been observed at lower latitudes around the equinoxes and 1-2 months later at mid-latitudes. In particular the temperature minimum systematically observed at the altitude of ~80 km and propagating downward throughout the night might also suggest the important role played by the tides.

Keywords: lidar, temperature, inversion layers, temperature inversions, mesosphere, middle atmosphere, tides.

1. INTRODUCTION

The mesospheric temperature inversion layers have been frequently observed and identified since they were first detected [1]. They are characterized by an inversion of the vertical temperature gradient in the mesosphere from negative to positive. The most striking events are usually observed [2] at winter midlatitudes near 70 km with amplitudes (defined as the difference between the temperatures at the top and the bottom of the layer) reaching 40 K. Some inversion layers with weaker amplitudes were also observed at low- and midlatitudes near the equinoxes between 75 and 85 km by the Solar Mesospheric Explorer (SME) [3], the Improved Stratospheric And Mesospheric Sounder (ISAMS) and the Halogen Occultation Experiment (HALOE) onboard UARS [2], and by lidar [4]. At this time it is uncertain whether the higher altitude inversions and the lower altitude winter inversions have the same origin. Hauchecorne and Maillard [5] and more recently Leblanc [6] proposed a dynamical mechanism for the winter inversions at 70 km while chemical heating and tidal effects were proposed [7, 4] to explain their formation at 80-85 km.

New results from different lidar observations of the inversion layers will be presented in this paper. Section 2 will briefly describe the lidar instruments and the database utilized. In section 3 the observation of the inversions at mid- and lower latitudes will be reported. Then we will focus on the winter inversions observed above Table Mountain Facility (TMF, 34.4°N) and investigate a possible tidal signature. It is suggested in the discussion (section 4) that pure tidal oscillations or gravity wave and tides coupling are both serious candidates for the formation of the inversions.

2. INSTRUMENTS AND DATA SETS.

The results presented here have been obtained using temperature measurements from four ground-based Rayleigh lidars located at mid- and low-latitudes. The CNRS-Service d'Aéronomie lidar at the Observatoire de Haute-Provence, France (OHP , 44°N, 6.0°E) has operated since 1978 and a second lidar at the Centre d'Essais des Landes (CEL, 44°N, 1.0°W) was operated between 1986 and 1994. These lidars typically made measurements all night long (approximately 6 to 12 hours a night) on 4-5 nights a week depending on the season and weather permitting. The Jet Propulsion Laboratory (JPL) has operated lidars at the Table Mountain Facility, California (TMF, 34.4°N, 117.7°W) since 1988 and at Mauna Loa, Hawaii (MLO, 19.5°N, 155.6°W) since 1993. Both JPL lidars routinely make a 2 hour measurement early in the night, 4 nights a week, with some additional full night campaigns in 1996, 1997, and 1998. Measurements from 1244 nights at OHP, 670 nights at CEL, 686 nights at TMF, and 411 nights at MLO were used to obtain the climatological results presented below. Two of the JPL lidar full night campaigns performed at TMF in January 1997 and February 1998, leading to a total of 140

hours of nighttime measurements distributed between ~19:00 and ~5:00 LST have been used to investigate the tidal signature in the winter midlatitude temperature inversions.

Basically, the lidars transmit a laser into the atmosphere where it is Rayleigh backscattered by the air molecules. The intensity of the backscattered radiation received by a telescope on the ground is proportional to the number of molecules, i.e. the air density. The temperature is then deduced from the density using the classic hydrostatic equilibrium and ideal gas law assumptions. The potential 20 K total error at the top of the profiles (principally due to the use of a priori information and to the low signal at the top) decreases rapidly to a few kelvins 10 km below, and to a few tenths of kelvins 20 km below. The instrument specifications and principle have already been extensively documented [8].

3. DATA ANALYSIS AND RESULTS

3.1 Climatology of the temperature inversions.

Figure 1 shows 9 nightly mean temperature profiles taken between December 1 and 10, 1991, at OHP (44°N). The shaded area represents the temperature plus and minus its calculated total error. The dashed lines indicate the monthly temperature climatology for December taken from CIRA-86 [9]. A strong temperature inversion can be seen to develop near 70 km starting on December 2, reaching a very large 55 K amplitude on December 5, then weakening and almost disappearing on December 10. This illustrates the magnitude and day-to-day variability of such winter inversions. Lifetimes of a few hours to a few days have been reported in the past [2].

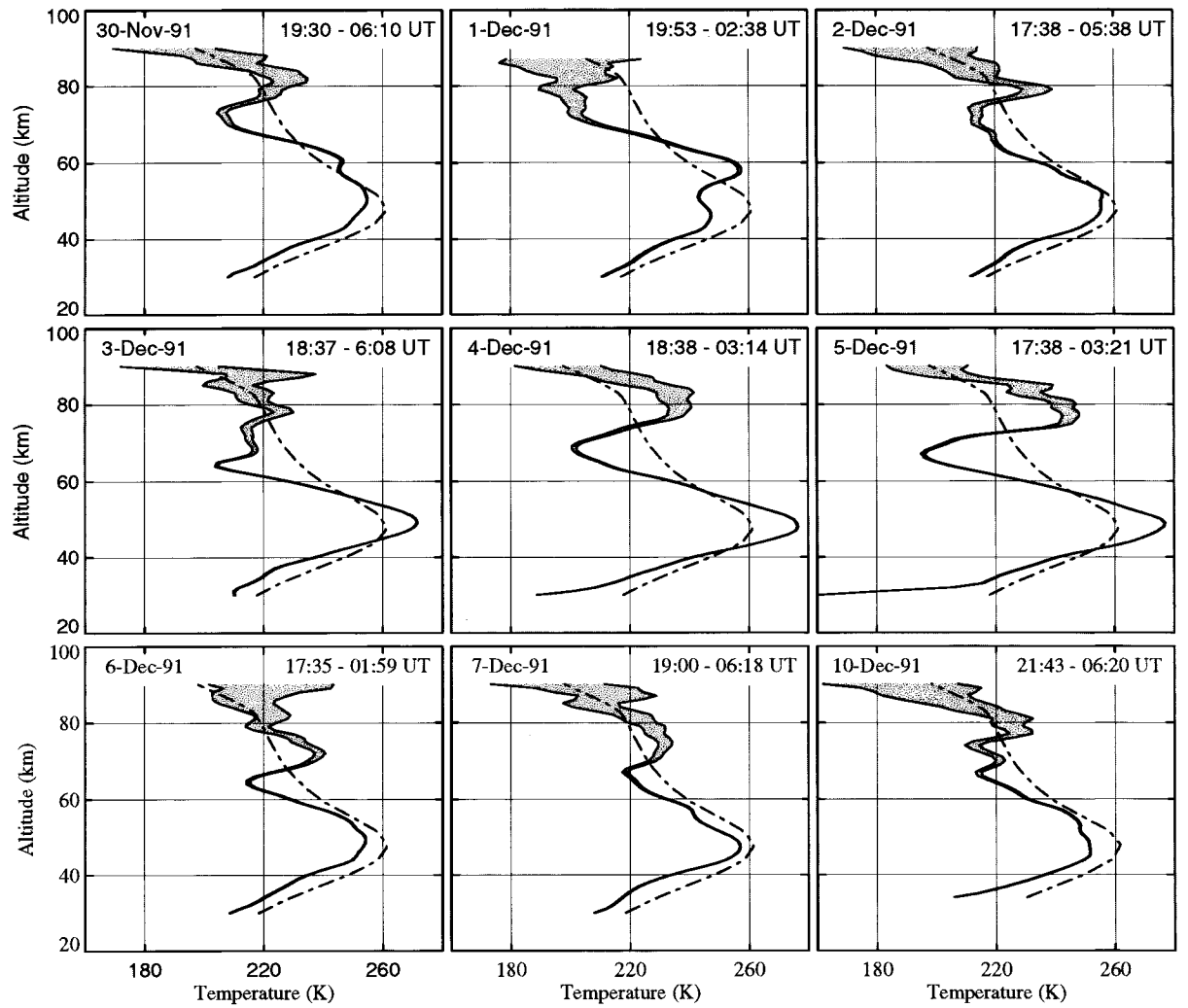

Figure 1. Nightly mean lidar temperature profiles between November 30 and December 10, 1991 over OHP (44.0°N). Integration times run from 6 h 45 min to 12 h depending on weather conditions. The dashed line is the CIRA-86 profile.

The nighttime evolution of a winter inversion at TMF (34.4°N) is illustrated in Figure 2 for the night of January 10, 1997. The temperature profiles are plotted every 1 hour and shifted by 10 K/hour to illustrate the time evolution. The first profile was taken at the very beginning of the night and the last profile at the very end. The total time separating the first and last profiles is approximately 12 hours. An important modulation of the amplitude (minimum of 10 K, maximum of 27 K) and an apparent downward propagation throughout the night are evident. These two characteristics are found almost every time. Occasionally (not shown here) the top of the inversion has been observed to propagate upward during short periods. The approximate downward phase speed of the inversion is 0.3 to 0.5 km/hour (8 to 14 cm.s^{-1}).

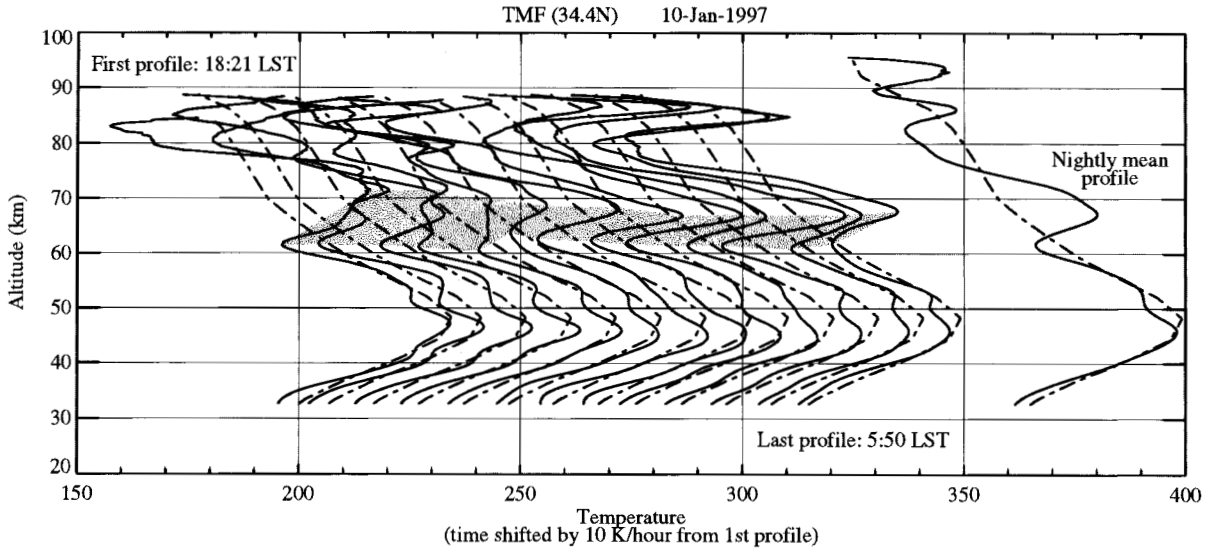

Figure 2. Hourly mean temperature profiles over TMF (34.4°N, 117°W) for January 10, 1997. Each profile is right-shifted by 10 K/hour, starting at 2:11 UT, ending at 13:40 UT. The dotted-dashed lines are the CIRA-86 climatology for January at the latitude of TMF. The lidar profile on the right-hand side is the nightly mean profile.

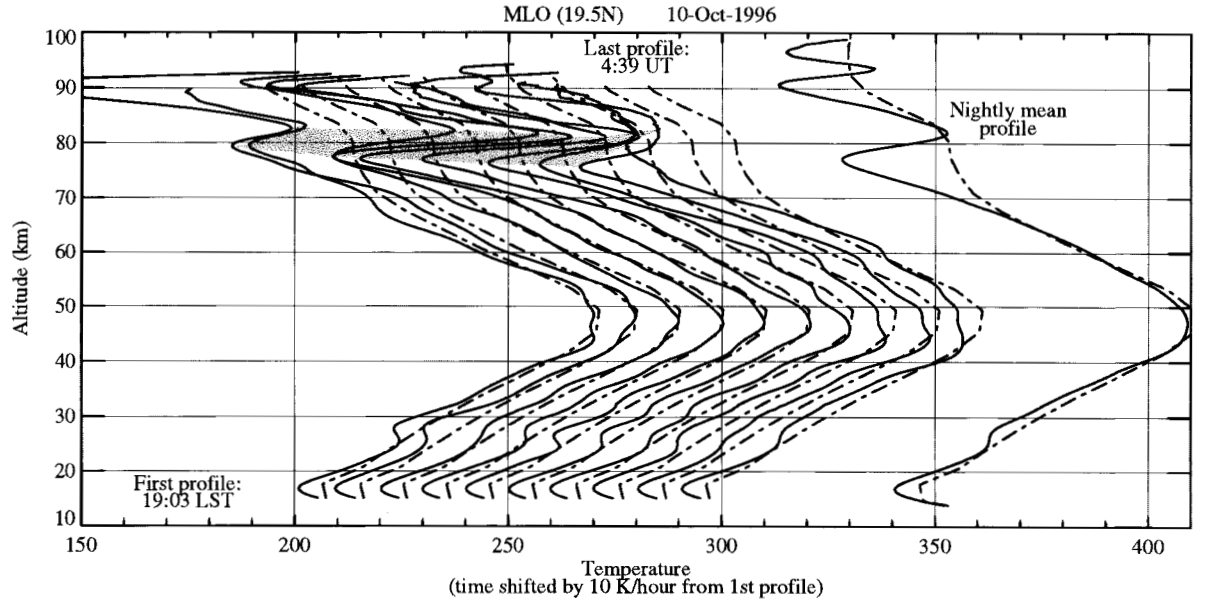

Figure 3. Same as figure 2, but over MLO (19.5°N, 155°W) for October 10, 1996. Starting and ending times are 5:25 UT and 15:01 UT. The dotted-dashed lines are the CIRA-86 climatology for October at the latitude of MLO.

Figure 3 shows the nighttime evolution of a temperature inversion observed at MLO (19.5°N) on October 10, 1996. In contrast to the winter inversions observed near 65-70 km at OHP and TMF, this inversion takes place near 80 km. The 40 K amplitude observed here is larger than the typical 10-20 K more frequently observed at this altitude. A downward propagation throughout the night is clearly observed. Some similar low-latitudes lidar observations of temperature inversions

have been reported previously by Dao et al [10]. Although their calculations were presented for a single day only (October 21, 1993), they inferred that the vertical phase speed and vertical wavelength of ~20 km corresponded to a diurnal tide.

Figures 4 (a) to (d) show the climatological average of the amplitude of the inversions as a function of altitude and season, observed at OHP (a) between 1984 and 1995, at CEL (b) between 1986 and 1994, at TMF (c) between 1990 and mid-1997, and at MLO (d) between mid-1993 and mid-1997. The altitude of the inversions is defined here as the center of the inversion layer. In order not to introduce errors due to the a priori initialization, the search for inversion layers was performed only up to about 10 km below the actual top of the profiles. This leads to top altitudes around 82 km for OHP, CEL, and MLO, and 78 km for TMF. At mid- and subtropical latitudes (i.e. OHP, CEL and TMF), the amplitude of the inversions at 70 km follows a well defined annual cycle with a maximum in winter. The winter maximum at TMF occurs 1 month later than at OHP and CEL (in January-February instead of December-January). This was already observed in a recent temperature climatology [11]. At 80 km a larger but narrower maximum is observed in October-November that is well separated from the winter inversions, especially at OHP. Though they appear to be separated from the winter inversions in Figure 4, it was shown [11] that the warm winter midlatitudes mesosphere starts up in early November around 80 km altitude. Then a warming period propagate downward from 80 km in early November to 70 km in late January [11]. Although also seen in the TMF results, this October-November maximum is to high to be observable in Figure 4. At MLO, the winter inversions are almost absent. Instead, a well defined semiannual cycle is observed at 80 km with maxima around the equinoxes. Despite some occasional altitude shifts these results are in good agreement with the satellite observations from SME [3], and ISAMS and HALOE [2].

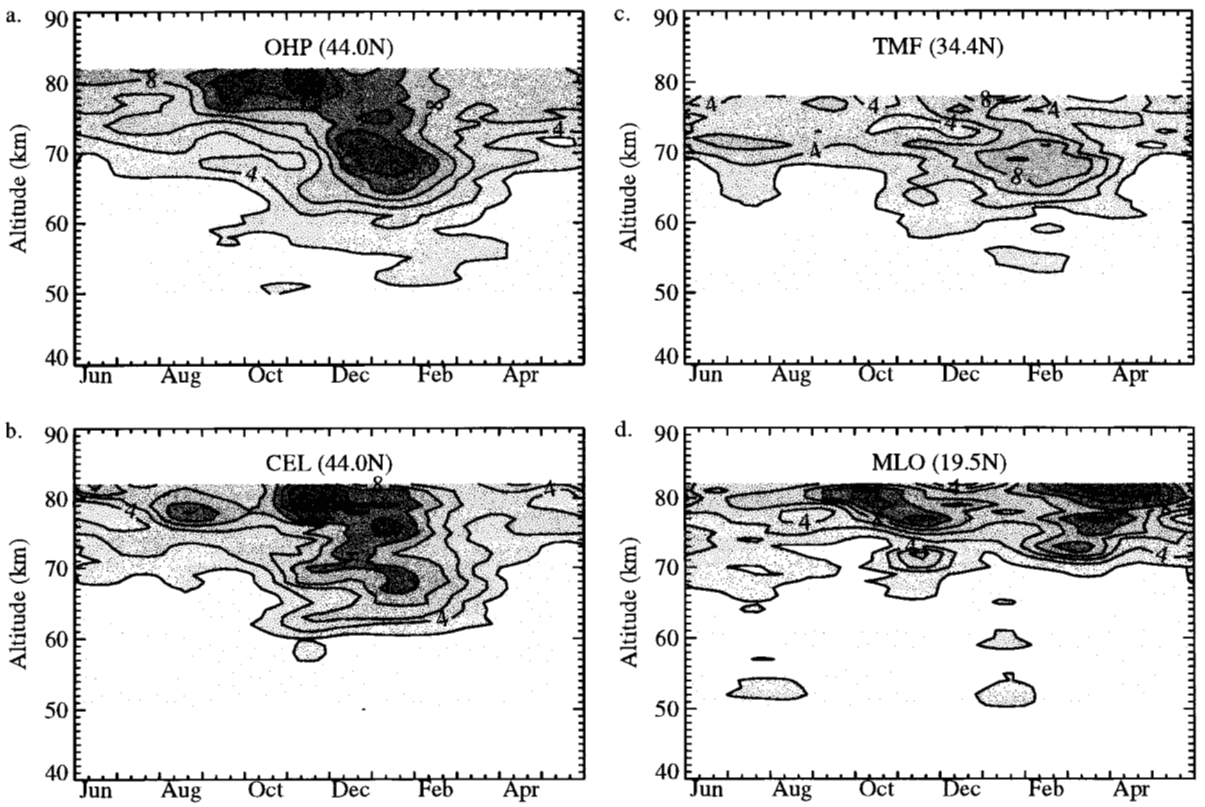

Figure 4. Monthly mean amplitude (K) of the mesospheric inversion layers as a function of season and altitude for a) OHP, b) CEL, c) TMF and d) MLO.

3.2 Nighttime evolution of the mesospheric temperature inversions.

Lidar temperature profiles obtained during 5 nights from January 7-11, 1997, and 7 nights between February 26 and March 4, 1998 were used to investigate the relationship between the temperature inversions and the Local Solar Time (LST). A total of 140 hours of lidar measurements distributed from 18:00 to 5:00 LST were available (maximum of 11-hours of continuous measurements per night). The raw lidar data for each of the 5 nights of January 1997 were combined to obtain mean nighttime profiles for January 1997, sampled every hour between 18:00 and 5:00 LST. The same method was employed to obtain mean nighttime profiles for February 1998, and similarly profiles combining January 1997 and February 1998. For the

three periods defined above, the nightly average profile was subtracted from each of the hourly mean profiles. The temperature differences obtained in February 1998 every hour between 18:00 and 5:00 LST are contoured as a function of altitude and time in Figure 5. For brevity, only the results from February 1998 will be shown. A very similar behavior has been observed in January 1997. A well defined thin layer of strong temperature change between 60 and 70 km, can be observed in figure 5, the result of the downward propagating temperature inversions. Also well defined is a wide layer of continuous cooling between 40 and 60 km and highly consistent with previous observations at winter midlatitudes [12]. The temperature differences observed by lidar were compared to the corresponding values calculated from the outputs of tidal models. The diurnal and semidiurnal phases and amplitudes from GSWM [13] were used to compute the GSWM temperature differences from nighttime average. These differences predicted by GSWM in January at the latitude of TMF are plotted in figure 6 with the same scales as figure 5. This way, the lidar results can be directly compared to GSWM. Since it has frequently been found that observed diurnal and semidiurnal amplitudes and those predicted by GSWM differ by at least a factor of two [10, 14, 4], the differences plotted in Figure 6 were determined by doubling the GSWM values. Remarkable similarities are found between the lidar and GSWM results. The warm early night and cold late night observed between 40 and 60 km is predicted by GSWM but between 40 and 55 km. The cold early night and warm late night observed by lidar in the thin layer 65-70 km (result of the downward propagating temperature inversion) is also predicted between 55 and 65 km by GSWM but with a much smaller amplitude. This last result would indicate that the mesospheric temperature inversions observed above TMF in winter are the result of the combined effect of the diurnal and semidiurnal components. Finally, although some geophysical and instrumental noise remains above 75 km in the lidar data it seems that the beginning of the night is warmer than the end of the night, especially in January 97 (not shown). This is still observed in February 98 but with a weaker amplitude. Again this is in good agreement with GSWM which predicts a larger effect of the semidiurnal component in January than in April (not shown).

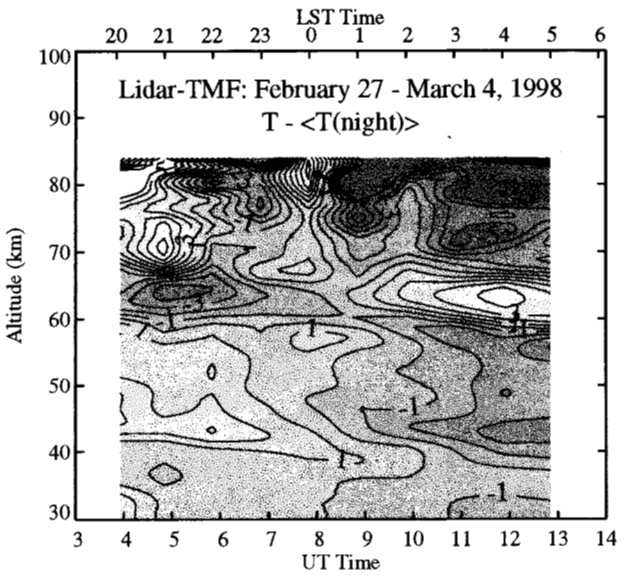

Figure 5. Hourly-mean lidar temperature differences from the nighttime average calculated for the 7 nights of February 1998 taken together.

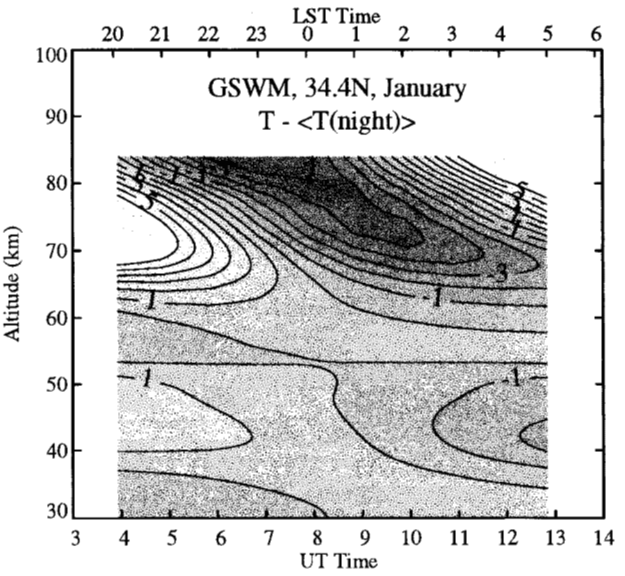

Figure 6. Same as figure 5 but the temperature differences were calculated using the phases and twice the amplitudes of the diurnal and semidiurnal components predicted by GSWM at 34.4°N in January.

4. DISCUSSION AND CONCLUSION.

Figures 1 to 6 in this paper reveal three principal results:

1) The observations of the inversion layers above TMF (34.4°N) and MLO (19.5°N) are in very good agreement with the previous observations and climatologies obtained by lidar, SME, ISAMS, and HALOE at similar latitudes [2, 3].

2) There appear to be at least two distinct types of inversions:

- The first are the winter mid-latitude inversions occurring near 70 km altitude in December-January above OHP and CEL (44°N) and 1- to 2-months later above TMF (34.4°N). The winter inversions have previously been observed many times in both Northern and Southern hemispheres by SME, ISAMS, and HALOE [2, 3].

- The second type of inversions occurs at higher altitudes (80-85 km) at the equinoxes above MLO (19.5°N). Many inversion layers have also been observed at these altitudes and at the equinoxes by SME, ISAMS, and HALOE at low latitudes, with a maximum amplitude at the equator[2].

- A possible third kind of inversion has been observed in October-November near 80 km above OHP, CEL, and TMF. These inversions appear to be well separated from those occurring at 70 km in winter and it is not clear whether they belong to the first type (winter midlatitude inversions) or to the second (equinox inversions), or even to a third type

3) The winter inversions above TMF have been found to be strongly LST-dependent, with some remarkable qualitative similarities in the resulting thermal structure with the tidal model GSWM.

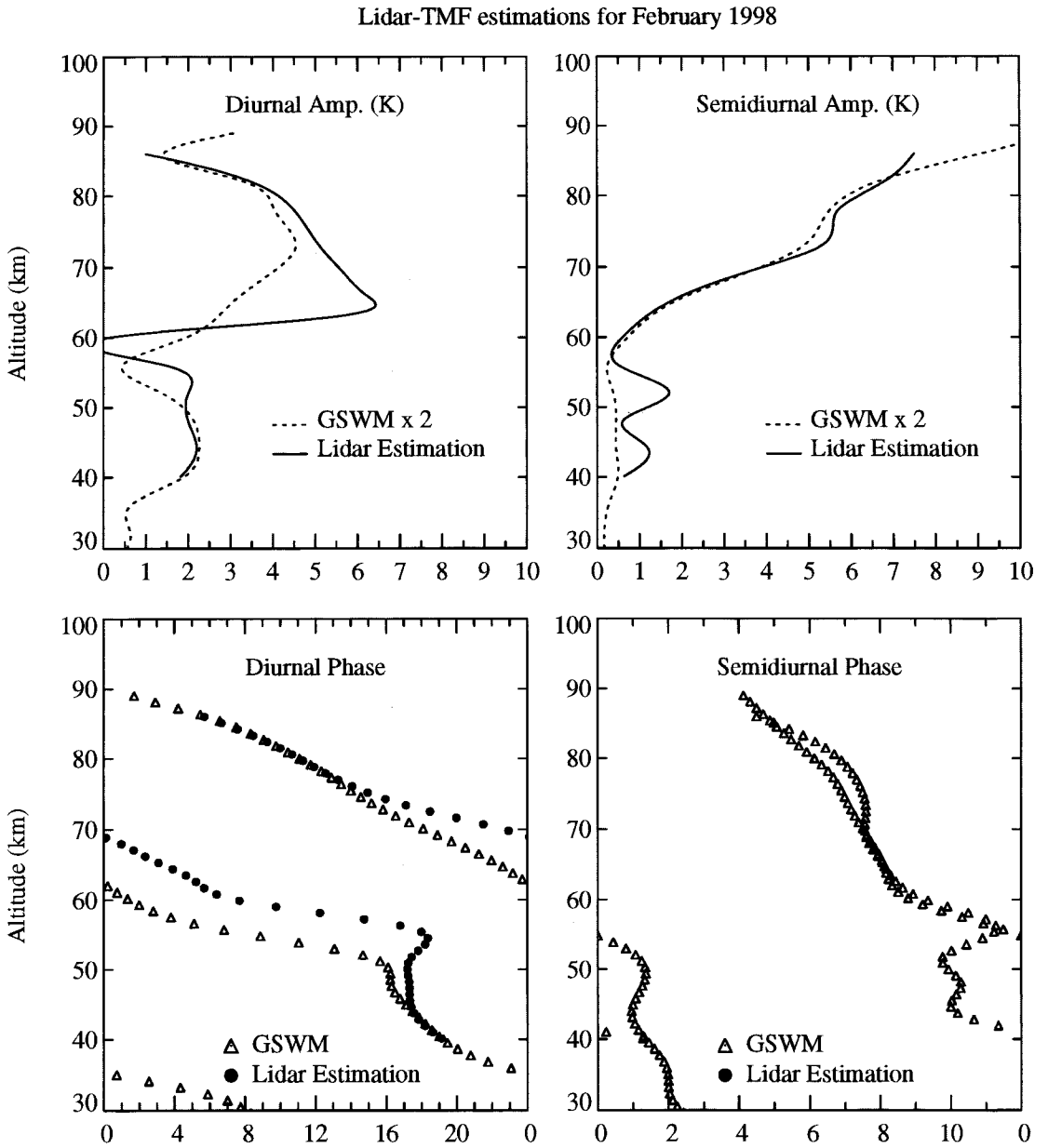

Figure 7. Diurnal (left) and semidiurnal (right) amplitudes (top) and phases (bottom) estimated from the February 1998 lidar measurements at TMF (solid lines and circles) and predicted by GSWM at 34.4°N in January (dotted lines and triangles).

Despite some important quantitative disagreement, result 3) would suggest that the middle atmospheric tides play a key-role in the formation or at least in the modulation of the temperature inversions. The logically occurring question is: Is this layer the result of a purely tidal signature, or is there a local effect (such as a 24-h period gravity wave forced in the lower

atmosphere), or could it be the result of coupling between gravity waves and tides? The suggestion of a local effect seems to be less probable since the temperature inversions and their LST-related behavior have been frequently observed at different locations [2, 4, 15] preferentially suggesting a more global effect. Therefore in the following discussion, we will focus only on the possible effect of pure tidal oscillations and on the possible effect of gravity wave-tidal coupling.

Assuming that the lidar observations in the mesosphere and, in particular, the temperature inversions are representative of a pure tidal signature, a major theoretical barrier has to be overcome. How large can the diurnal and semidiurnal amplitudes be at 70 km altitude to lead to inversions with frequent 25 K amplitudes? Using a "first guest" method and using simulated data, the diurnal and semidiurnal phases and amplitudes have been estimated using the nighttime lidar profiles. A detailed method for the estimation of the tidal components has been recently presented by Leblanc [16] . While the semidiurnal component remains smaller than the diurnal component (especially below 70 km) and consequently could not be correctly estimated in the entire middle atmosphere, the diurnal component has been clearly identified. The diurnal and semidiurnal component estimated from the lidar observations are plotted in figure 7 together with that of GSWM. It appears that the estimated diurnal amplitude and phase are qualitatively close to those calculated by GSWM but shifted by a few kilometers in altitude. In particular, the fast phase transition calculated to be around 58 km by GSWM and corresponding to the transition between the upper stratospheric forced (trapped) modes and the upward propagating modes has been estimated using the lidar data to be around 63 km, i.e., ~5 km higher. Immediately above this altitude the warm late night following the cold early night is the consequence of a fast growing diurnal amplitude with height. However, this behavior is contained in only a 5-8 km thin layer because of the emergence of the semidiurnal component at upper altitudes. This latter together with the diurnal component is responsible for the warm early night then cold late night observed between 70 km and 75 km. The estimated diurnal amplitude has a minimum at 58 km (transition between trapped and propagating modes) and a maximum of 6.5 K at 65 km, with an associated phase around 2:00 LST. The diurnal amplitude calculated by GSWM has its minimum at 56 km and a maximum of 2.5 K around 72 km. The estimated semidiurnal phase is close to that of GSWM, with still a factor of two between the calculated and estimated amplitudes. Thus, using estimated components qualitatively close to those calculated by GSWM it is possible to reproduce adequately the nighttime behavior of the temperature inversions. The cold bottom part of the inversion is mainly governed by the diurnal oscillation while the warm top part of the inversion is actually governed by both the diurnal and semidiurnal oscillations. Above 75 km, the semidiurnal component is dominant and leads to a cold midnight and warm late night above 80 km. The resulting temperature profile above 75 km therefore shows the downward propagation of a second inversion with its bottom observable at the end of the night in some of the lidar profiles around 80 km altitude (not shown).

Although it has been shown that it is at least qualitatively possible to explain the formation of the temperature inversions with the effect of pure tidal oscillations, the alternative explanation of a gravity wave-tidal coupling is not unlikely. Indeed, using 2D numerical modeling Liu and Hagan [17] have shown that the altitude and severity of the gravity wave breaking and its consequences can be strongly influenced by the background wind, especially the tidal wind. The gravity wave breaks preferentially in the region of strong vertical shear with the same sign as that of the gravity wave phase speed. Then, turbulence, diffusion and advection lead to cooling and heating layers, following the same mechanisms as in previous modeling of gravity wave-mean flow interaction [18, 5, 19]. The difference to previous modeling is the LST dependence of the vertical shear (or in case of wave overturning the suradiabatic temperature gradient) and consequently the LST dependence of the formation of the inversions. This LST- and, especially, gravity wave-related mechanism would clarify two major striking features which have not been elucidated previously. The strong day-to-day variability observed in many cases and the large amplitudes, sometimes reaching 35-40 K at winter midlatitudes [2]. In addition, the simulations are able to produce a second temperature inversion (multiple breaking levels) located one vertical wavelength higher which is consistent with the observations [4]

At this time, there are no available observations capable of favoring either of the two possible mechanisms described above for the formation of the winter midlatitude temperature inversions. The similarities between the observations and the outputs from GSWM are remarkable but there is still a large disagreement in the amplitudes involved to assert that purely tidal oscillations are responsible for the formation of the temperature inversions. On the other hand, numerical modeling has shown that LST-dependent temperature inversions can develop after gravity breaking but the mechanistic model used in that case is at an early stage of development and more simulations have to be made to locate and quantify more precisely the resulting mesospheric heating and cooling. In contrast, the higher altitude inversions (85-90 km) occurring at lower latitudes during the equinoxes and at mid-latitudes 1-2 months later may be more directly tidal related. Their observed seasonal variations and amplitudes are more consistent with the tidal theory. For both winter inversions and high altitude inversions it is probable that several mechanisms interact with each other. More temperature measurements in the mesosphere, in particular over full 24-hour cycles, are necessary to refine our estimations of the thermal tidal components and have a better

understanding of the middle atmospheric thermal structure. The future development of daytime lidar measurement techniques and long-term satellite measurements may hopefully bring new answers.

ACKNOWLEDGEMENTS

The work described in this paper was carried out, in part, at the Jet Propulsion Laboratory, California Institute of Technology, under an agreement with the National Aeronautics and Space Administration. The long term measurements at OHP and CEL have been supported by DRET, CNES and INSU for CNRS.

REFERENCES

1. F. J. Schmidlin, "Temperature inversions near 75 km", *Geophys. Res. Lett.*, *3*, pp. 173-176, 1976.
2. T. Leblanc, and A. Hauchecorne, "Recent observations of the mesospheric temperature inversions", *J. Geophys. Res.*, **102**, pp. 19,471-19,482, 1997.
3. R. T. Clancy, D. W. Rush, and M. T. Callan, "Temperature minima in the average thermal structure of the middle atmosphere (70-80 km) from analysis of 40- to 92-km SME global temperature profiles", *J. Geophys. Res.*, **99**, pp. 19,001-19,020, 1994.
4. R. J. States, and C. S. Gardner, "Influence of the diurnal tide and thermospheric heat sources on the formation of mesospheric temperature inversion layers", *Geophys. Res. Lett.*, **25**, pp. 1483-1486, 1998.
5. A. Hauchecorne, and A. Maillard, "A 2-D dynamical model of mesospheric temperature inversions in winter", *Geophys. Res. Lett.*, **17**, 2197-2200, 1990.
6. T. Leblanc, "Observation et modélisation numérique des inversions mésosphériques de température", *Ph.D. Thesis*, pp. 1-258, *Université Pierre et Marie Curie, Paris 6*, July 1995.
7. J. W. Meriwether, and M. G. Mlynczak, "Is chemical heating a major cause of the mesosphere inversion layer ?", *J. Geophys. Res.*, **100**, pp. 1379-1387, 1995.
8. T. Leblanc, T., I. S. McDermid, A. Hauchecorne, and P. Keckhut, "Evaluation and optimization of lidar temperature analysis algorithms using simulated data", *J. Geophys. Res.*, **103**, pp. 6177-6187, 1998.
9. E. L. Fleming, S. Chandra, J. J. Barnett and M. Corney, "COSPAR International Reference Atmosphere, Chapter 2: Zonal mean temperature, pressure, zonal wind and geopotential height as functions of latitude", *Adv. Space Res.*, **10 (12)**, pp. 11-59, 1990.
10. P. D. Dao, R. Farley, X. Tao, and C. S. Gardner, "Lidar observations of the temperature profile between 25 and 103 km: evidence of strong tidal perturbation", *Geophys. Res. Lett.*, **22**, pp. 2825-2828, 1995.
11. T. Leblanc, I. S. McDermid, C. Y. She, D. A. Krueger, A. Hauchecorne, and P. Keckhut, "Temperature climatology of the middle atmosphere from long-term lidar measurements at mid- and low-latitudes", *J. Geophys. Res.*, (in press), 1998.
12. S. T. Gille, A. Hauchecorne, and M. L. Chanin, "Semidiurnal and diurnal tidal effects in the middle atmosphere as seen by Rayleigh lidar", *J. Geophys. Res.*, **96**, pp. 7579-7587, 1991.
13. M. E. Hagan, J. M. Forbes and F. Vial, "On modeling migrating solar tides", *Geophys. Res. Lett.*, **22**, 893-896, 1995.
14. J. Yu, R. States, S. J. Franke, C. S. Gardner and M. Hagan, "Observations of tidal temperature and wind perturbations in the mesopause region above Urbana, IL (40°N, 88°W)", *Geophys. Res. Lett.*, **24**, pp. 1207-1210, 1997.
15. J. W. Meriwether, X. Gao, V. B. Wickwar, T. Wilkerson, K. Beissner, S. Collins, and M. E. Hagan, "Observed coupling of the mesosphere inversion layer to the thermal tidal structure", *Geophys. Res. Lett.*, **25**, pp. 1479-1482, 1998.
16. T. Leblanc, I. S. McDermid, and D. A. Ortland, "Lidar observation of the middle atmospheric thermal tides. Comparison with HRDI and GSWM. Part I: Methodology and winter observations over Table Mountain (34.4°N)", *J. Geophys. Res.*, (submitted), 1998.
17. H.-L. Liu, and M. E. Hagan, "Local heating/cooling of the mesosphere due to gravity wave and tide coupling", *J. Geophys. Res.*, (submitted), 1998.
18. J. R. Holton, "The influence of gravity wave breaking on the general circulation of the middle atmosphere", *J. Atmos Sci.*, **40**, pp. 2497-2507, 1983.
19. D. C. Fritts, J. F. Garten and Ø. Andreassen, "Wave breaking and transition to turbulence in stratified shear flows", *J. Atmos. Sci.* **53**, pp. 1057-1085, 1996.